energies

Article

Multi-Objective Optimization of Insulation Thickness with Respect to On-Site RES Generation in Residential Buildings

Agis M. Papadopoulos [1,*], Konstantinos Polychronakis [2], Elli Kyriaki [1] and Effrosyni Giama [1]

[1] Process Equipment Design Laboratory, Department of Mechanical Engineering, Aristotle University, 54124 Thessaloniki, Greece; kelli@auth.gr (E.K.); fgiama@auth.gr (E.G.)
[2] Department of Mechanical Engineering, National Technical University of Athens, 15772 Athens, Greece; polichronakis_konstantinos@mail.ntua.gr
* Correspondence: agis@auth.gr

Abstract: This paper investigates the optimization of insulation thickness with respect to the integration of renewable energy systems in residential buildings in order to improve energy efficiency, maximize the contribution of renewables and reduce life cycle costs. Using the DesignBuilder and EnergyPlus software, this study models a representative two-story residential building located in Athens, Greece. The building envelope features extruded polystyrene thermal insulation and windows with unplasticized polyvinyl chloride frames and low-e glazing. Six scenarios with hybrid renewable energy systems are analyzed, including air- and ground-source heat pumps, solar thermal systems and a biomass fired boiler, so as to assess energy consumption, economic feasibility and internal air temperature conditions. A Pareto-fronts-based optimization algorithm is applied to determine the optimal combination of insulation thicknesses for the walls, the roof and the floor, focusing on minimizing the life cycle cost and maximizing the percentage of renewable energy utilized. The results demonstrate that scenarios involving biomass boilers and solar thermal systems, both for heating and cooling, when combined with reasonable thermal protection, can effectively meet the recent European Union's directive's goal, with renewable energy systems contributing more than 50% of the total energy requirements, whilst maintaining acceptable internal air temperature conditions and having a life cycle cost lower than contemporary conventional buildings.

Keywords: thermal insulation; renewable energy; energy efficiency; optimization

Citation: Papadopoulos, A.M.; Polychronakis, K.; Kyriaki, E.; Giama, E. Multi-Objective Optimization of Insulation Thickness with Respect to On-Site RES Generation in Residential Buildings. *Energies* **2024**, *17*, 5609. https://doi.org/10.3390/en17225609

Academic Editor: Matteo Manganelli

Received: 22 September 2024
Revised: 3 November 2024
Accepted: 5 November 2024
Published: 9 November 2024

1. Introduction

In the European Union (EU), for the year 2022, residential buildings accounted for approximately 26% of the total final energy consumption and services, which, to a large extent, is also taking place in other buildings, accounting for another 14% [1]. The first Energy Performance of Buildings Directive was introduced in 2001, aiming at using less and cleaner energy whilst improving indoor environmental conditions [2]. Still, the increasing environmental burden, the rise in fuel prices, especially since the geopolitical instability due to the war in the Ukraine, and the dependency on supplier countries have led to the necessity of reaching the levels of nearly zero-energy buildings, both in new constructions and, by means of refurbishment, in the building stock, given the fact that 75% of European buildings still have low energy efficiency [3]. Towards this direction, three important directives were adopted by the European Parliament in the last two years: (a) the revised Energy Performance of Buildings Directive (EU/2024/1275), aiming to achieve a fully decarbonized building stock by 2050, (b) the revised Energy Efficiency Directive (EU/2023/1791), introducing the 'energy efficiency first' as a fundamental principle of EU energy policy, giving it legal standing for the first time and (c) the revised Renewable Energy Directive (EU/2023/2413), establishing an overall renewable energy target of at least 42.5% for by 2030 but aiming for 45%. These directives are for Europe, and, hence, also for Greece, and they are significant milestones on the path to carbon neutrality by 2050 [4]. Furthermore, when studying the directives in detail, one cannot fail to notice that EU policy focuses not only on the upgrading building efficiency but also, in a more holistic approach, raising the quality of living for people in the buildings, as well as improving the urban environment [5]. According to the latest statistics mentioned in the directive, two-thirds of the energy used to heat and cool buildings still comes from fossil fuels. Natural gas plays the largest role in heating buildings, accounting for around 39% of the energy used for space heating in the residential sector. Oil is the second most important fossil-based heating fuel, accounting for 11%, while coal accounts for about 3%. It is therefore understood that the gradual abolition of fossil fuels in the heating and cooling sector is of particular importance for the decarbonization of the building sector. Member States should phase out conventional boilers, and, as a first step, no financial incentives should be provided for the installation of these boilers, while it should still be possible to provide financial incentives for the installation of hybrid heating systems with a significant share of renewable energy, such as combinations of a boiler with solar thermal energy or a heat pump [6]. So, in order to accomplish the required reduction in carbon emissions by up to or more than 80% and simultaneously increase energy efficiency, the share of renewable energy systems (RES) implemented in the energy sector and, more specifically, in the building sector should be increased [7]. More specifically, the large-scale application of hybrid renewable energy systems is a key parameter in achieving zero carbon emissions, so renewable energy sources must satisfy building energy demands [8]. Moreover, a prerequisite for this strategy is also the limitation of the use of fossil fuels in electricity generation. In Greece, significant progress has been made over the past decade; in 2023, renewables accounted for 45% of the total electricity generation, and when counting big hydroelectric plants, this figure reached 57% [9], compared to less than 15% in 2010. However, it is clear that there are more challenges associated with the electrification of heat, especially in terms of the transition from conventional heating technologies to renewable energy systems, which, in some cases, may require an expanded electricity infrastructure, which could result in high initial investment costs [10]. Also, control systems will play a significant role in reducing energy consumption, so attention should be given to finding optimal control systems, especially when hybrid renewable energy systems are considered, so as to ensure that the efficiency of the RES system is maximized and that the maximum possible RES energy is used. Moreover, the integration of control systems in RES systems would ensure that there would be more efficient collaboration between energy storage, the system itself and the demand, which would again lead to a more efficient system overall [11]. However, control systems on their own are not enough. In order to ensure power system stability, more sophisticated and complex control techniques, like the demand response, are required, in order to provide flexible solutions to the inelastic demand side. The incorporation of RES in power systems enhances the existing issues associated with grid operation due to their unpredictability and intermittency, and this is why the demand response technique is investigated as a solution to fixing or eliminating these problems [12].

Hybrid renewable energy systems with or without thermal energy storage, as well as hybrid combined heat and power renewable energy systems, are a vivid research field. Daneshazarian and Berardi studied a hybrid renewable energy system consisting of photovoltaic collectors for covering electricity demand, vacuum tube collectors and a ground-source heat pump. This system was combined with an underground thermal energy storage system with nanomaterials so as to increase its energy efficiency. The results showed that the incorporation of the nano-enhanced thermal energy storage system increased the overall performance of the hybrid system by 27.1%, and the energy consumption was reduced by 36.7% [13]. In another research work, Wang et al. investigated a combined system where solar thermal collectors, photovoltaic panels, a hot water storage tank, a battery and a diesel engine were installed in a residential building. The solar thermal system was used to produce domestic hot water, space heating and space cooling by using an absorption refrigeration system. It was concluded that after the optimal design of the proposed system, the internal temperature of the studied residential building was controlled, and thermal comfort was achieved [14]. A hybrid system with photovoltaic panels, a wind turbine, a ground-source heat pump, a fuel cell, a diesel generator and a battery was examined by Cheraghi and Jahangir. More specifically, they implemented a multi-objective optimization analysis of the aforementioned system, which was installed in a residential building. It was seen that the power system that used only the diesel engine as a backup source had a lower levelized cost of energy but higher carbon dioxide emissions. Additionally, they stated that fuel cells are an expensive technology but have many environmental advantages [15]. Moreover, Jaffarian et al. performed a multi-objective optimization analysis of a hybrid energy system for residential buildings. More specifically, different energy storage systems (a latent thermal energy storage system with phase-change materials, hydrogen storage with fuel cells and battery storage with Li-On cells) combined with renewable energy sources (photovoltaic/thermal collectors, heat pumps and a desiccant wheel) were studied. It was calculated that, in warm climates, a renewable energy fraction of 85.35% can be achieved, while in cold climates, a renewable energy fraction of 59.23% can be achieved, leading to 1088.24 kWh and 731.37 kWh annual electricity savings, respectively [16]. Last but not least, a novel solar–biomass micro combined heat and power system for residential applications was studied by Skiadopoulos et al. The proposed system covered 97.10% and 25.85% of the annual demand for space heating and electricity, respectively. In addition, the annual carbon footprint of the studied building was reduced by 31.22 kg equivalent carbon dioxide (CO_{2eq}), while the annual primary energy saving was 46.58 kWh/m^2 after the implementation of the proposed system [17].

Within the framework of this paper, strategies for optimizing insulation thickness and integrating renewable energy sources to improve energy efficiency and reduce life cycle costs (LCCs) in residential buildings are studied. Utilizing state-of-the-art simulation tools such as DesignBuilder V7.0.2.006 which uses EnergyPlus V9.4.0.002 sourced by Gloucestershire, United Kingdom, this study models a two-story residential building located in climate zone B. This study evaluates various combinations of insulation and RES to determine solutions that not only achieve optimal thermal comfort but also align with the EU's directive requiring a minimum of 49% renewable energy integration [18]. By systematically analyzing and optimizing different scenarios, this study aims to provide actionable insights for enhancing residential energy systems and meeting stringent energy performance standards, thereby supporting the broader goals of sustainable building practices and regulatory compliance.

With respect to the scenarios examined, following reasons led to choosing the specific systems: There are a great variety of RES systems that one can examine, and within the limited space of a paper, we focused on combinations that are currently usually used in Greece. Solar thermal systems are the most popular RES system in urban areas and the most widespread RES system in the Greek building sector due to the country's favorable climate conditions and the presence of a strong industry since the 1970s. They have the highest acceptance rate by the public and are therefore the primary option for hot water production and supporting space heating systems. Heat pumps are becoming gradually more popular, despite their high initial costs. Biomass-fired boilers are not used in urban areas due to their emissions and due to practical problems, like the lack of storage space for pellets. They are, however, used in suburban and rural areas. Furthermore, natural gas will act as a bridge fuel towards the climate neutrality target and will remain the conventional mainstay in the coming two decades for residential heating, both alone and as a back-up system.

The use of building applied photovoltaics undoubtedly has benefits and is an appealing option. In this paper, however, we focused on the use of thermal RES (solar thermal, biomass, geothermal energy) as part of the effort to support heating and cooling decarbonization, which accounts for a large proportion of the energy consumption in European households. The 'electrification' of buildings' heating systems is a parallel track to meeting this goal, and there is strong interest in it, which is expressed in many research projects and the resulting literature.

Furthermore, this study's results can be used for the calculation and improvement of the smart readiness indicator of residential buildings, an indicator which will be mandatory in the next years. The smart readiness indicator of buildings assesses the technological readiness of a building by evaluating the functionality level of various smart devices, aiming at energy savings, the ability of the building to respond to users' needs and energy flexibility [19]. Last but not least, it is worth noting that there are many papers in the literature regarding the calculation of the optimal insulation thickness for various building elements [20], but investigations into the optimal insulation thickness in relation to the achieved renewable energy percentage are missing.

2. Materials and Methods

The computational analysis was conducted using the DesignBuilder V7.0.2.006 software which uses EnergyPlus V9.4.0.002, sourced by Gloucestershire, United Kingdom, for the energy simulation This study focused on a two-story residential building with a ground floor and two similar upper levels, as illustrated in Figure 1. The building was located in Athens, which belongs to climate zone B according to the Greek National Legislation [21]. The total conditioned floor area was 876.9 square meters, with a conditioned volume of 2178.3 cubic meters. The building was oriented to the north, and the window-to-wall ratio was approximately 30%.

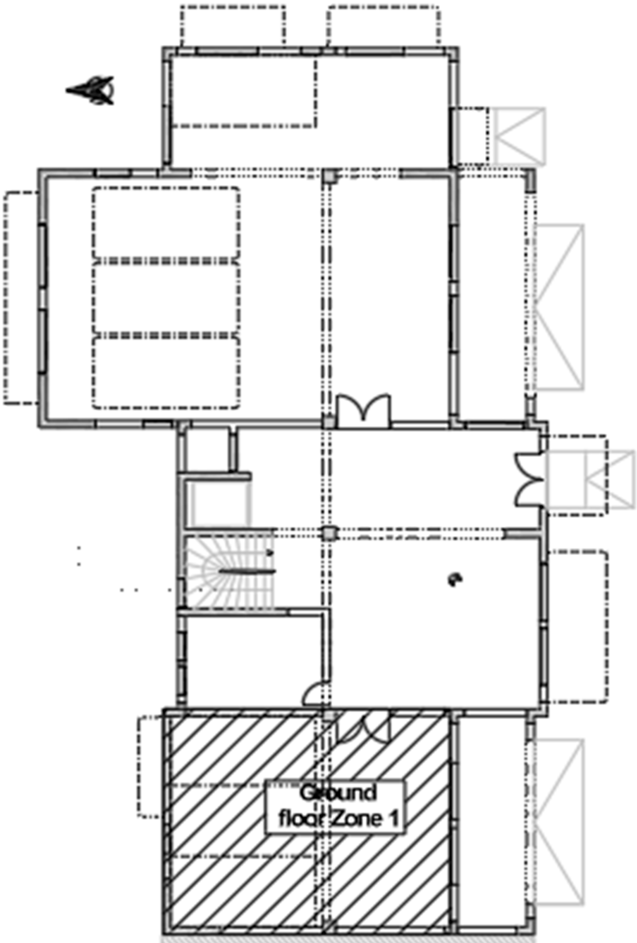

(a)

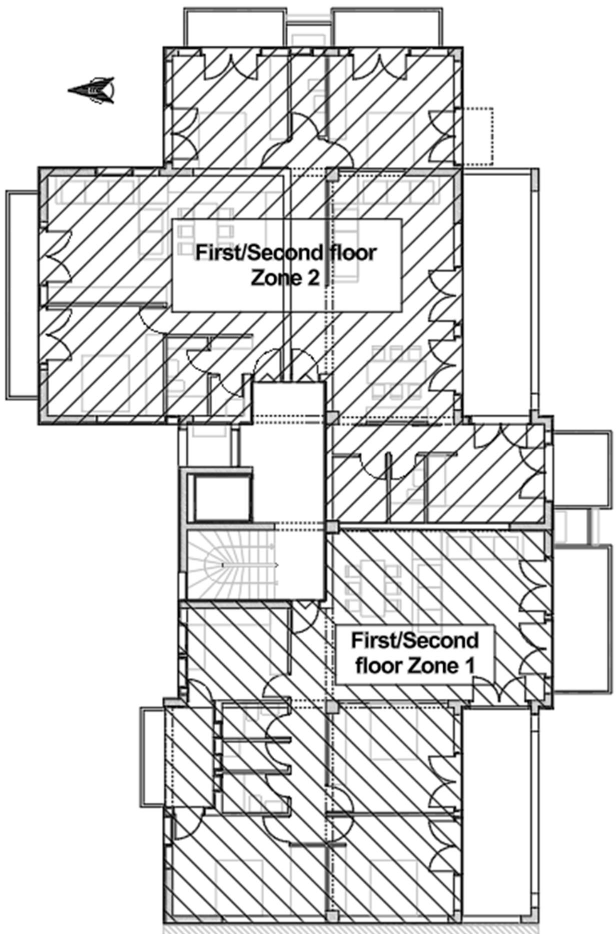

(b)

Figure 1. (**a**) Ground floor, (**b**) first/second floor.

The building was initially modeled based on provided architectural designs, and then the structural elements were defined, and the appropriate materials were selected to minimize thermal losses. So, extruded polystyrene was used to insulate the external walls, roof and floor, with a thermal conductivity coefficient $\lambda = 0.033[\mathrm{W/mK}]$ [22]. Also, triple-glazed windows were used with $U_{glazing} = 0.8\left[\mathrm{W/m^2K}\right]$. Regarding the window frame, unplastic polyvinyl chloride (UPVC) material was selected, with a U-value of $U_{window\ frame} = 1.6\left[\mathrm{W/m^2K}\right]$. Furthermore, regarding the demand for lighting, it was assumed that most rooms needed between 200–300 lux illuminance, which was covered by light-emitting diode (LED) lamps of 2.5 $\mathrm{W/m^2}$ each. After the modeling of the building, the next step was to select the heating, ventilation and air conditioning (HVAC) systems. In this study, the calculations regarding the internal conditions were based exclusively on the internal air temperature within the building's thermal zones. The indoor temperature was maintained between 22 °C and 24 °C during summer and between 19 °C and 21 °C during winter. External factors, such as radiant heat gains or losses, were excluded from the assessment to ensure consistency across all scenarios. This approach focused on stabilizing the internal air temperature as the primary metric, which allowed for a controlled comparison of the different energy supply systems, independent of the outdoor environmental conditions. In every scenario, a steady-state heating design analysis was performed to calculate the maximum heating load of the building, and a steady-state cooling design analysis was performed to calculate the maximum cooling load. To ensure consistency in comparing the impacts of the various energy supply methods on the building's cooling and heating loads, an initial sizing of each HVAC system was conducted using the uninsulated building model as a baseline. This baseline allowed for a standardized calculation of the heating and cooling load requirements, facilitating a uniform starting point for assessing the different energy systems. For each subsequent scenario that included various insulation thicknesses, the *autosize* function was employed. This function dynamically adjusted the capacity of each HVAC system to match the specific heating and cooling demands created by the different insulation levels, ensuring that each system's output power was aligned with the corresponding load. By maintaining the initial sizing based on an uninsulated structure and employing the *autosize* adjustment for each insulation variant, the analysis was conducted on a comparable scale. This methodology allowed for consistent evaluation across the energy supply methods while accounting for variations in the building envelope performance and its influence on operational costs.

To calculate renewable energy integration, six different scenarios of hybrid systems were studied with different combinations of boilers, heat pumps, solar thermal systems and solar absorption chillers. In this analysis, the price of electricity was assumed to be 0.12 EUR/kWh, and the prices for biomass (pellet) were set at 0.11 EUR/kWh and 0.085 EUR/kWh, depending on the source. In Table 1, the technical characteristics of each scenario are presented.

2.1. Detailed HVAC Modeling

In every scenario, a detailed HVAC model was designed to appropriately size each part of the system, with the main goal of achieving acceptable internal conditions within the building. The controlled parameter was the air temperature in each thermal zone, which was divided into five distinct areas, with the first on the ground floor and the others on the first and second floors, corresponding to the four apartments. The heating setpoint was established at 20 °C and the cooling setpoint at 24 °C based on values from the Greek legislation of the Technical Chamber of Greece for residential buildings in climate zone B [23]. To optimize the system performance and maintain stable conditions, a hysteresis of ±2 °C was implemented. Consequently, the heating system was set to activate when the temperature falls below 18 °C and deactivate when it exceeds 22 °C. Similarly, the cooling system was set to begin operation when the temperature rises above 26 °C and stop when it drops below 22 °C.

Table 1. Technical specifications of the HVAC systems for each scenario.

Case	Heating	Cooling	Domestic Hot Water	Technical Specifications
1	Biomass boiler, 20 m^2 solar collector	Local air conditioning units	20 m^2 solar thermal collector, biomass boiler as auxiliary source	40 kW Boiler 89% efficiency EERlocal units = 3
2	Water-to-water geothermal heat pump, condensing natural gas boiler as auxiliary source	Water-to-water geothermal heat pump	20 m^2 solar thermal collector thermal, condensing natural gas boiler as auxiliary source	COP = 4, EER = 5.5, Pheating = 10 kW Pcooling = 9 kW
3	Air-to-air heat pump, condensing natural gas boiler as auxiliary source	Air-to-air heat pump	20 m^2 solar thermal collector, condensing natural gas boiler as auxiliary source	COP = 3.2, EER = 4, Pheating = 16 kW Pcooling = 13 kW
4	Air-to-water heat pump, condensing natural gas boiler as auxiliary source	Local air conditioning units	20 m^2 solar thermal collector, condensing natural gas boiler as auxiliary source	COP = 4.5, Pheating = 11 kW EERlocal units = 3 Pcooling = 16 kW
5	160 m^2 solar collector, biomass boiler as auxiliary source	Solar absorption chiller	20 m^2 solar thermal collector, biomass boiler as auxiliary source	30 kWbBoiler 89% efficiency 55 kW solar absorption chiller COP = 0.85
6	Water-to-air geothermal heat pump	Water-to-air geothermal heat pump	20 m^2 solar thermal collector	COP = 3, EER = 4.5, Pheating = 15 kW Pcooling = 12 kW

2.2. Optimization Algorithm

The optimization process utilized the JEA optimization engine, which offers a range of configurable parameters to fine-tune the performance and effectiveness of the search for optimal solutions. The generation population size determines the number of solutions evaluated per iteration, with larger populations generally required for more design variables and influenced by the number of available processor cores. As the Pareto archive builds, the max population size limits the number of solutions per generation. The crossover rate, set high at 1.0, combines genetic information from parent solutions to create new offspring, mimicking biological crossover. The mutation rate, with a default of 0.4, ensures genetic diversity and helps prevent premature convergence, balancing the need for fast convergence and thorough exploration of parameter space. The tournament size, typically set to 2, governs the selection process, where larger sizes reduce the chance of weak individuals being selected, thus pushing towards desired objectives more effectively. The objective bias setting controls the trade-off between the Pareto ranking and constraint feasibility. Additionally, the optimization can be constrained by the max evaluations and max wall time, ensuring the process halts after a specified number of iterations or hours, respectively, preventing excessive computational time and resources from being expended unnecessarily. In this study, a Pareto-front-based optimization algorithm was employed to determine the optimal combination of the insulation thickness, RES integration and life cycle cost (LCC). The objective function used was the minimization of the LCC and the maximization of the RES, considering a 20-year life cycle and the percentage of RES integration [24]. Two different optimization algorithms were used in this study, one for the scenarios that included a heat pump and a second one for the scenarios that included a boiler. However, in all scenarios, the equations used regarding domestic hot water, lighting, equipment fans and pumps were the same.

2.2.1. Equations for the Heat Pump Scenarios

The energy performance of the heat pump scenarios was calculated by Equations (1)–(8).

$$E_{HP,C} = \frac{Q_C}{EER}\ [\text{kWh}] \tag{1}$$

$$E_{HP,H} = \frac{Q_H}{COP}\ [\text{kWh}] \tag{2}$$

$$E_{HP,Total} = E_{HP,C} + E_{HP,H}\ [\text{kWh}] \tag{3}$$

$$RES_{HP,C} = Q_C - E_{HP,C}\ [\text{kWh}] \tag{4}$$

$$RES_{HP,H} = Q_H - E_{HP,H}\ [\text{kWh}] \tag{5}$$

$$RES_{Total,HP} = RES_{HP,H} + RES_{HP,C}\ [\text{kWh}] \tag{6}$$

$$RES_{Total} = RES_{HP,H} + RES_{HP,C} + RES_{DHW}\ [\text{kWh}] \tag{7}$$

$$Q_{Total} = E_{HP,Total} + Q_{DHW} + Q_L + Q_E + E_{pumps} + E_{fans}\ [\text{kWh}] \tag{8}$$

2.2.2. Equations for the Boiler Scenarios

Moreover, Equations (9)–(12) were used to calculate the energy performance of the boiler scenarios.

$$Q_B = \frac{Q_H}{n_B}\ [\text{kWh}] \tag{9}$$

$$RES_{Biomass} = Q_H\ [\text{kWh}] \tag{10}$$

$$Q_{Total} = Q_B + Q_C + Q_{DHW} + Q_L + Q_E + E_{pumps} + E_{fans}\ [\text{kWh}] \tag{11}$$

$$RES_{Total} = RES_{Biomass} + RES_{DHW}\ [\text{kWh}] \tag{12}$$

2.2.3. Domestic Hot Water Equation

The percentage of RES regarding DHW was calculated by Equation (13).

$$RES_{DHW} = Q_{DHW} - E_{DHW}\ [\text{kWh}] \tag{13}$$

2.2.4. Total Renewable Percentage Equation

The overall RES percentage was estimated by Equation (14).

$$RES_{\%} = \frac{RES_{Total}}{Q_{Total}} \times 100\% \tag{14}$$

2.2.5. Life Cycle Cost Equation

Regarding the economic assessment, LCC was calculated by Equation (15).

$$LCC = C_{initial} + \sum_{t=1}^{n} \frac{\left(C_{O,t} + C_{M,t} + C_{replacement,t}\right)}{(1+r)^t} - \frac{R_{end}}{(1+r)^n}\ [€] \tag{15}$$

2.2.6. Initial Cost Equation

The initial Cost was estimated by Equation (16).

$$C_{initial} = C_{external\ walls} + C_{internal\ walls} + C_{windows\ frame} + C_{windows\ glazing} + C_{lighting} + C_{insulation} + C_{HVAC}\ [€] \tag{16}$$

2.2.7. HVAC Cost Equation (Ground-Source Heat Pumps Cases)

The HVAC cost for the ground source heat pump scenarios was calculated by Equation (17).

$$C_{HVAC} = C_{purchase} + C_{drilling}\ [€] \tag{17}$$

2.2.8. Operational Cost Equation

The operational cost was calculated by Equation (18)

$$C_{O,t} = C_{HVAC,t} + C_{lighting,t} + C_{devices,t}\ [€] \tag{18}$$

2.2.9. HVAC Operational Cost Equation (Only Electricity)

The HVAC operation cost, only for electricity, was estimated by Equation (19).

$$C_{HVAC,t} = E_{HVAC} \times C_{electricity,t} \ [€] \tag{19}$$

2.2.10. HVAC Operational Cost Equation (Electricity and Biomass)

The HVAC operational cost both for electricity and biomass was estimated by Equation (20).

$$\begin{gathered} C_{HVAC,t} = \left(E_{cooling} + E_{pumps} + E_{fans} + E_{DHW}\right) \times C_{electricity,t} \\ +(E_{heating}) \times C_{biomass,t} \ [€] \end{gathered} \tag{20}$$

2.2.11. Objective Function and Constraints

The objective function and the constraints are presented in Equation (21).

$$\begin{gathered} Min_{s_{walls}, s_{roof}, s_{floor}} \ (LCC - RES_{\%}) \\ subject\ to: \\ C_{initial} \leq \ C_{initial,max} \\ C_{O,yearly} \leq \ C_{O,yearly,max} \\ Q_{total} \leq \ Q_{total,max} \\ 0 \leq s_{walls} \leq 20 \text{ cm} \\ 0 \leq s_{roof} \leq 20 \text{ cm} \\ 0 \leq s_{floor} \leq 20 \text{ cm} \end{gathered} \tag{21}$$

2.2.12. Python Code for Data Extraction

A Python code was developed to extract data from an SQL database created after each EnergyPlus simulation. The code uses the simulation output file to consider every energy demand of the building. The workflow diagram of the code is presented in Figure 2.

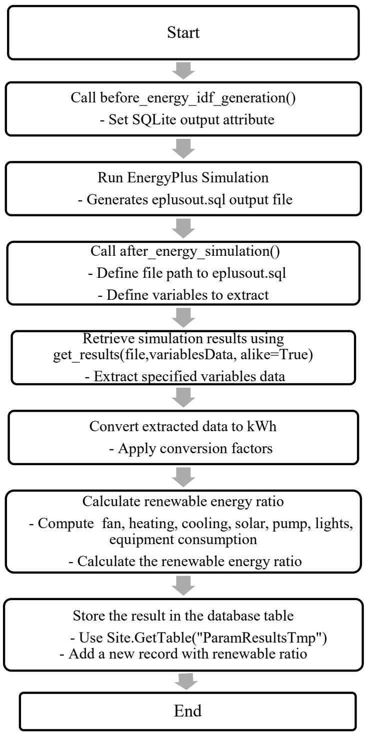

Figure 2. Workflow diagram of the Python script.

The script automates the process of extracting, processing and storing the energy consumption data from EnergyPlus simulations. By calculating the renewable energy ratio, it provides valuable insights into the sustainability and energy efficiency of the simulated building. This information can be crucial for designing energy-efficient buildings and optimizing their energy systems.

3. Results

The results of every optimization process indicate the optimal combination of the insulation thickness for the external walls, the ground floor and the roof of the building.

In Figures 3–7, the results for every scenario are shown.

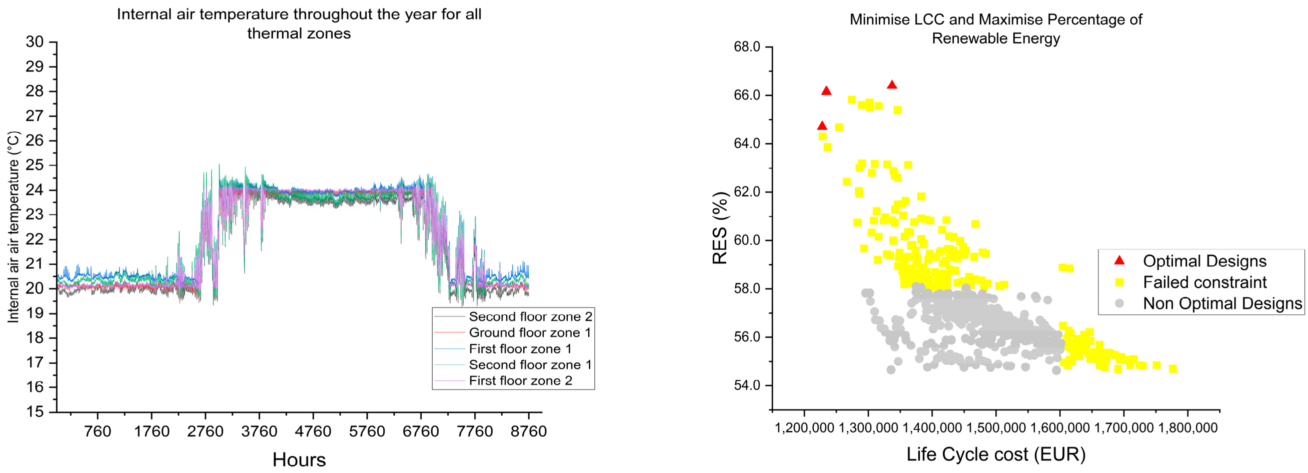

(**a**) (**b**)

Figure 3. (**a**) Internal air temperature throughout the year, (**b**) optimization results for Scenario 1.

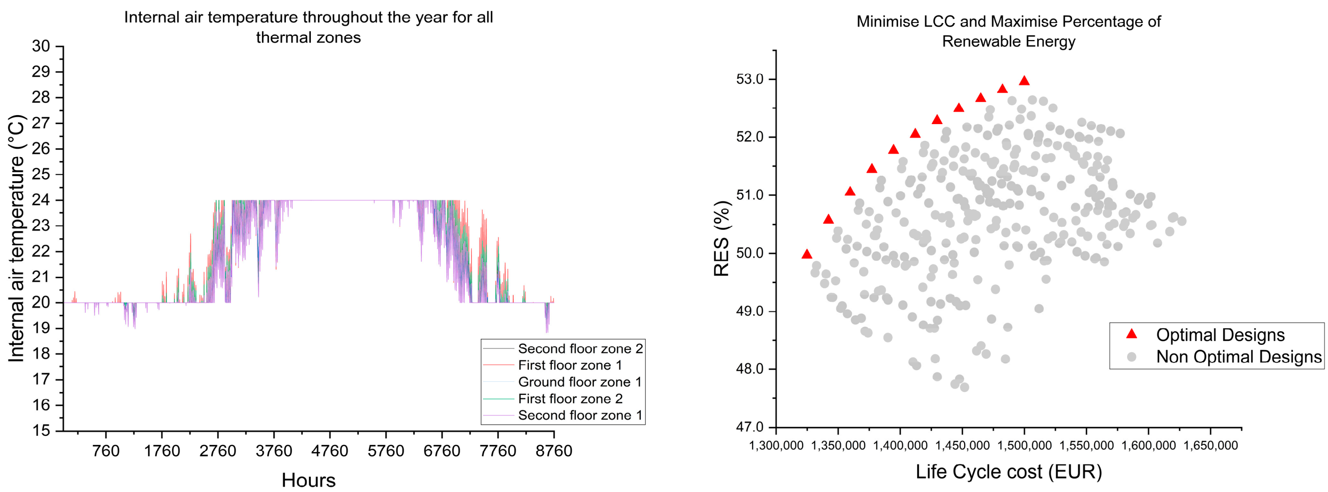

(**a**) (**b**)

Figure 4. (**a**) Internal air temperature throughout the year, (**b**) optimization results for Scenario 2.

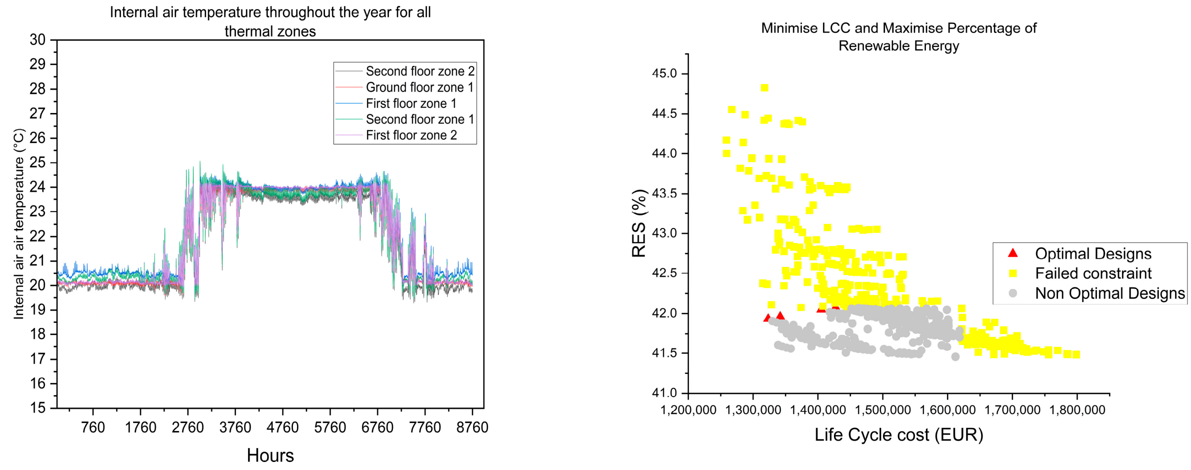

(**a**) (**b**)

Figure 5. (**a**) Internal air temperature throughout the year, (**b**) optimization results for Scenario 3.

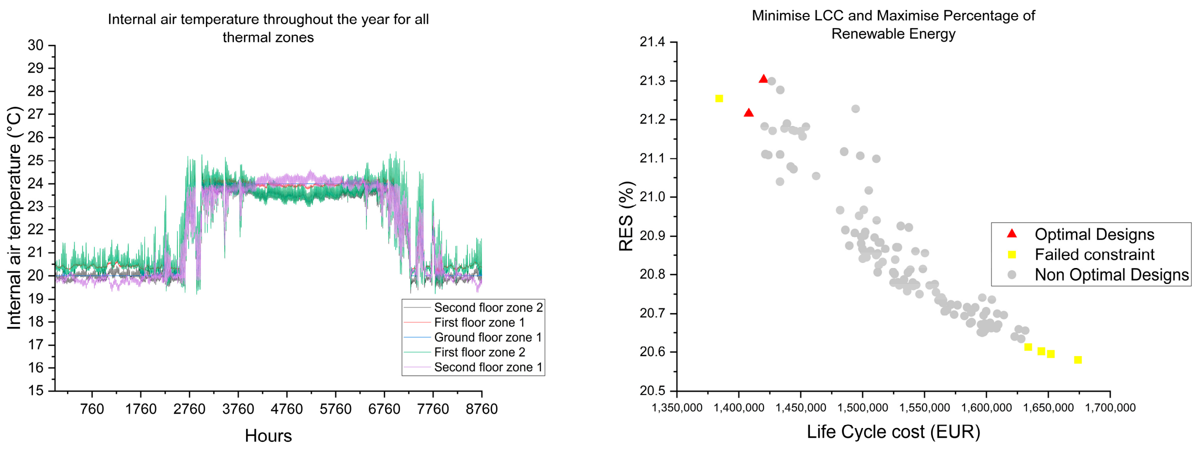

(**a**) (**b**)

Figure 6. (**a**) Internal air temperature throughout the year, (**b**) optimization results for Scenario 4.

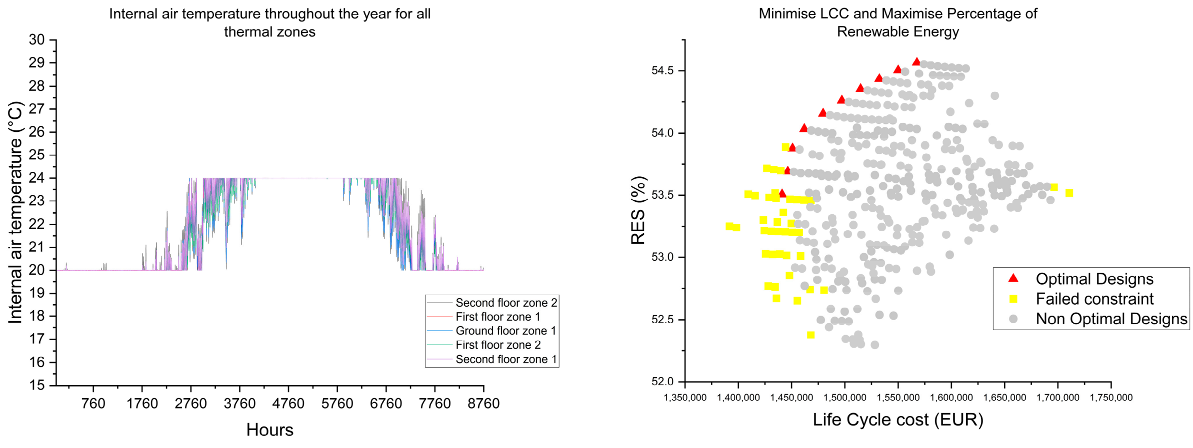

(**a**) (**b**)

Figure 7. (**a**) Internal air temperature throughout the year, (**b**) optimization results for Scenario 5.

3.1. Scenario 1: Biomass Boiler, Solar Thermal Collector and Packaged Terminal Air Conditioning Unit

In this case, the heating demand was effectively met by using a biomass boiler combined with floor heating as the terminal unit. The system maintained stable thermal comfort levels throughout the year. The cooling demand was covered by a packaged terminal air conditioning unit, which operated efficiently in all thermal zones. Domestic hot water requirements were fulfilled by a solar thermal collector equipped with an internal heating element. The integration of renewable energy reached approximately 65%, primarily due to the contribution of the biomass boiler. However, the optimization process revealed that several configurations exceeded the operational cost constraints and the construction cost constraints for insulation thicknesses over 16 cm.

3.2. Scenario 2: Ground-Source Water-to-Water Heat Pump and Solar Thermal Collector

In this scenario, the ground-source heat pump (GSHP) demonstrated stable performance in terms of both heating and cooling, while a low-temperature natural gas boiler was installed as a backup. Fan coil units were chosen as terminal units, allowing for the efficient management of heating and cooling. The optimization did not encounter any violations of constraints, mainly due to the reduced electricity consumption and operational costs achieved by the GSHP. This case effectively minimized operational costs while maintaining high energy efficiency.

3.3. Scenario 3: Air-to-Air Heat Pump and Solar Thermal Collector

This scenario, relatively unstable thermal comfort levels were obtained, though they were still within acceptable limits. The instability was attributed to the selected air system. Optimization attempts frequently failed to meet the operational cost constraints, primarily due to the significant electricity consumption caused by the heat pump's mechanical components, including the supply fan and the heating coil.

3.4. Scenario 4: Air-to-Water Heat Pump and Solar Thermal Collector

The air-to-water heat pump seemed to deliver very stable thermal comfort levels due to the usage of water convectors for heating and the packaged terminal air conditioning unit for the cooling demand. On the other hand, the renewable energy percentage was low because of the internal heating element in the heat pump that was necessary in order to cover the heating demand when the outside air temperature was low. So, it is obvious that in this case, the electricity consumption was increased, while the renewable energy percentage was reduced.

3.5. Scenario 5: Solar Absorption Chiller, Biomass Boiler and Solar Thermal Collector

The scenario with the solar absorption chiller had the most complex and detailed HVAC model. The solar thermal collectors' area (160 m^2) had multiple purposes; at first, it was used to cover the domestic hot water demand, and second it was used as a heating source for the solar absorption chiller, and it also participated in the coverage of the heating demand along with the biomass boiler. The optimization indicates a high renewable energy integration percentage with a small number of combinations failing the constraint of the operational costs. Additionally, the insulation thickness of over 13 cm also failed the constraint of the construction costs.

3.6. Scenario 6: Ground-Source Water-to-Air Heat Pump and Solar Thermal Corrector

Last but not least, the scenario with the water-to-air heat pump presented a relatively unstable performance (but between the acceptable margins) in terms of thermal comfort levels due to the air system being used as the terminal unit. As it can be seen in Figure 8, the renewable energy percentage was lower than the scenario with the water-to-water heat pump due to the required higher electricity consumption. The optimization indicates that the combinations with an insulation thickness of over 15 cm failed the constraint of the construction costs. The overall results regarding the optimal insulation thickness for each scenario are summarized in Table 2.

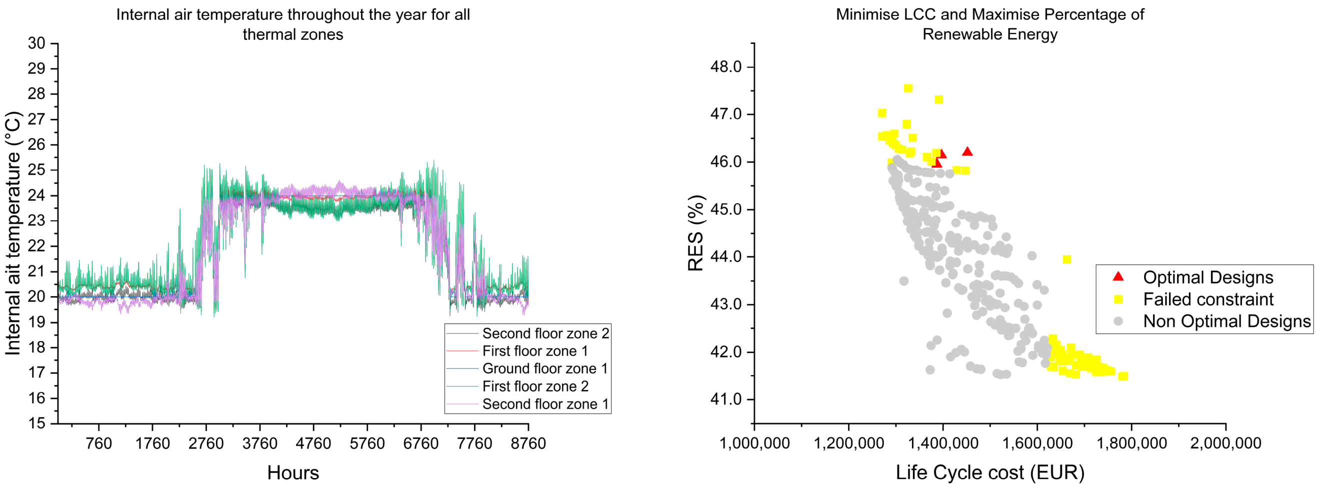

(**a**) (**b**)

Figure 8. (**a**) Internal air temperature throughout the year, (**b**) optimization results for Scenario 6.

Table 2. Optimal insulation thicknesses for external walls, roof and floor in every case.

Optimal Insulation Thickness			
Scenario	**External Walls [cm]**	**Roof [cm]**	**Floor [cm]**
Biomass boiler, solar collector and local air conditioning units	Varies from 0 to 3 cm	Varies from 0 to 8 cm	Varies from 5 to 15 cm
Water-to-water heat pump and solar thermal collector	Varies from 5 to 6 cm	Varies from 5 to 6 cm	Varies from 2 to 6 cm
Air-to-air heat pump and solar collector	Varies from 2 to 9 cm	Varies from 0 to 9 cm	Varies from 0 to 4 cm
Air-to-water heat pump and solar collector	Varies from 5 to 13 cm	Varies from 5 to 6 cm	Varies from 0 to 4 cm
Water-to-air heat pump, solar thermal collector and local air conditioning units	Varies from 6 to 12 cm	Varies from 4 to 5 cm	Varies from 6 to 9 cm
Solar absorption chiller, biomass boiler and solar thermal collector	Varies from 5 to 8 cm	Varies from 7 to 15 cm	Varies from 5 to 6 cm

4. Discussion

In Figure 9, it is clearly shown that the scenarios (a) with the biomass boiler, (b) with the solar absorption chiller combined with a biomass boiler and (c) with the solar thermal collectors and the water-to-water heat pump could meet the EU directive's goal of 45% renewable energy integration. The water-to-air heat pump achieved a slightly lower percentage of renewable energy integration due to the required additional fan systems powered by electricity, but it still stands as an excellent option because of its low operational costs and stable performance. The air-to-air heat pump and the air-to-water heat pump seemed to have the lowest integration of renewable energy due to the significantly higher electricity consumption.

Furthermore, in Figure 10, the economic feasibility of each scenario is presented based on the life cycle analysis. It is obvious that the scenario with the biomass boiler had the lowest life cycle costs. On the other hand, the most cost-intensive solution was the solar absorption chiller due to its significantly lower COP and its high initial investment costs. Regarding the heat pumps, it was observed that for all four scenarios, the differences were small. It was seen that the ground-source heat pumps had high initial investment costs, mainly due to drilling costs, whereas air-source heat pumps had higher operational costs due to the required electricity consumption when the outside temperature was low. Although the indoor and outdoor temperatures remained constant across all scenarios, the building envelope's performance had to be adjusted based on the characteristics of each energy supply system. Systems with higher operational efficiency, such as ground-source heat pumps, benefit from better insulation, as it helps to reduce operational costs by minimizing heat losses. Conversely, less efficient systems, like air-to-air heat pumps, result in higher electricity consumption, requiring adjustments to the envelope to balance the life cycle costs. Therefore, optimizing the building envelope directly contributes to lowering operational costs and ensuring that renewable energy systems can meet the desired energy targets while maintaining cost-effectiveness.

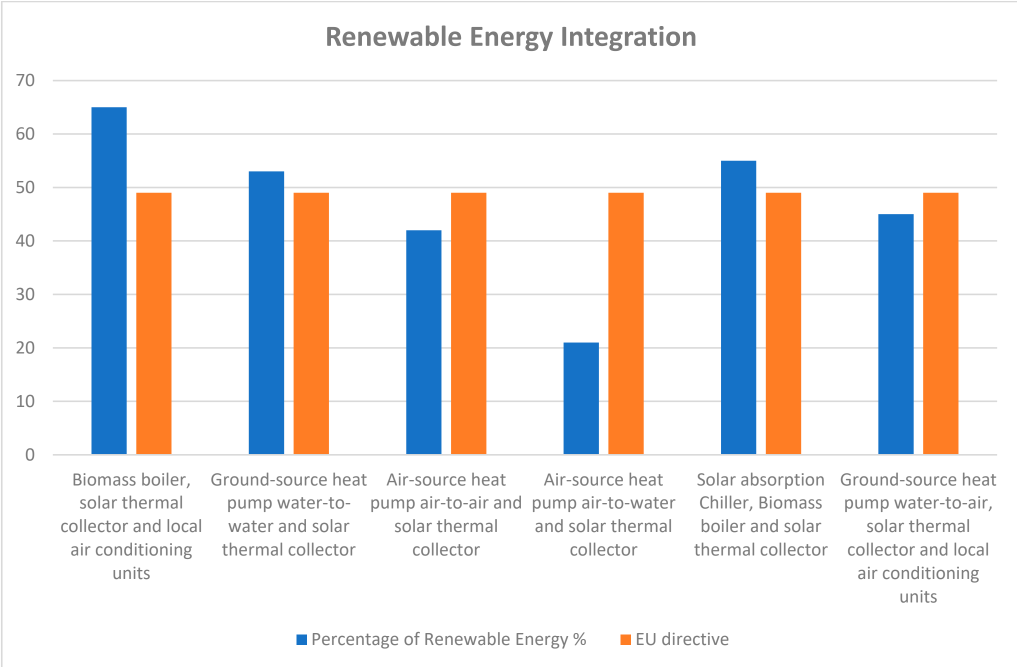

Figure 9. Comparison of each case with the EU directive.

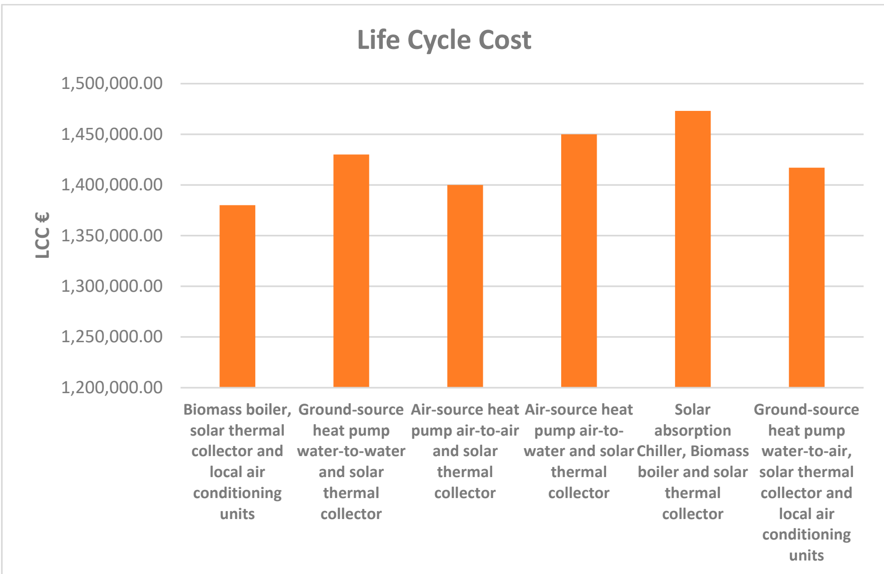

Figure 10. Comparison of life cycle costs for each scenario.

5. Conclusions

This research underscores the importance of optimizing insulation and incorporating renewable energy sources in residential buildings so as to maximize energy efficiency and cost savings. The use of advanced computational tools and optimization algorithms offers a robust framework for evaluating and implementing sustainable building solutions. The results highlight the importance of selecting appropriate materials and systems to enhance energy efficiency and economic feasibility. More specifically, regarding thermal insulation, it was observed that the optimal thermal insulation thickness in combination with the maximization of the RES integration varied from 0 cm up to 13 cm for external walls, 0–15 cm for roofs and 0–15 cm for floors, depending on the heating and cooling system. In terms of the energy simulations, it was found that thermal insulation was the variable with the largest effect on the energy consumption of the building. The increase in thickness limited the energy requirements for heating to a great extent, but at the same time, there was a slight increase in the cooling requirements, as heat transfer was minimized between the interior and exterior of the building. Based on the energy results regarding RES integration, it was concluded that the optimal solution was the biomass boiler. The ground-source heat pumps also had an equally high rate of RES integration along with a steady operation. On the other hand, the air-source heat pumps presented an unstable operation when the outside air temperature was low, and as a result, the RES integration percentage was reduced. Furthermore, regarding the calculated life cycle costs, the optimal scenario was once again the one with the biomass boiler, while the absorption chiller scenario was the worst. Additionally, the four heat pump scenarios presented similar results in the life cycle costs analysis with small differences. More specifically, the ground-source heat pumps had higher initial investment costs, whereas the air-source heat pumps had higher operational costs. Lastly, future research should investigate the integration of more renewable energy technologies like photovoltaics and/or micro wind turbines and, more importantly, hybrid solutions, including, for example, photovoltaics, heat pumps and storage, alongside their economic feasibility. Moreover, an environmental assessment should take place throughout the whole life cycle of the studied systems so as to include the environmental aspect in the analysis. Additionally, future studies should consider the variability in HVAC system performance ratios, specifically the efficiency, coefficient of performance and energy efficiency ratio, as these metrics respond to changes in a building's thermal envelope and different weather conditions across climate zones. This approach would provide a more nuanced understanding of energy supply optimization across diverse climates and building structures. Finally, incorporating thermal comfort metrics, such as the Predicted Mean Vote (PMV) and Predicted Percentage of Dissatisfied (PPD), would enable a comprehensive evaluation of occupant thermal comfort.

Author Contributions: Conceptualization, A.M.P., K.P., E.K. and E.G.; methodology, A.M.P., K.P. and E.K.; software, K.P. and E.K.; validation, A.M.P. and K.P. and E.G.; formal analysis, A.M.P., K.P. and E.K.; investigation, A.M.P. and K.P.; resources, A.M.P., K.P., E.K. and E.G.; data curation A.M.P. and E.K.; writing—original draft preparation, A.M.P., K.P., E.K. and E.G. writing—review and editing, A.M.P., K.P. and E.K.; visualization, A.M.P., K.P.; supervision, A.M.P.; project administration, A.M.P.; funding acquisition, A.M.P. All authors have read and agreed to the published version of the manuscript.

Funding: This research received no external funding.

Data Availability Statement: Data will be made available on request.

Conflicts of Interest: The authors declare no conflicts of interest.

Abbreviations

The following abbreviations are used in this manuscript:

EU	European Union
RES	Renewable energy systems
CO_{2eq}	Equivalent carbon dioxide [kg]
LCC	$Life\ cycle\ cost$ [EUR]
UPVC	Unplastic polyvinyl chloride
LED	Lighting-emitting diode
HVAC	Heating, ventilation and air conditioning
Q_H	$Annual\ heating\ load$ [kWh]
Q_C	$Annual\ coaling\ load$ [kWh]
Q_{DHW}	$Annual\ domestic\ hot\ water\ load$ [kWh]
Q_L	$Annual\ lighting\ energy\ consumption$ [kWh]
Q_E	$Annual\ equipment\ energy\ consumption$ [kWh]
EER	$Energy\ effiency\ ratio\ [-]$
COP	$Coefficient\ of\ perfomance\ for\ heating\ [-]$
n_B	$Efficiency\ of\ the\ boiler$
Q_B	$Boiler\ fuel\ consumption$ [kWh]
E_{pumps}	$Annual\ electricity\ consumption\ of\ pumps$ [kWh]
E_{fans}	$Annual\ electricity\ consumption\ of\ fans$ [kWh]
$E_{heating}$	$Annual\ electricity\ consumption\ for\ heating$ [kWh]
$E_{cooling}$	$Annual\ electricity\ consumption\ for\ cooling$ [kWh]
E_{DHW}	$Annual\ electricity\ consumption\ for\ domestic\ hot\ water\ [kWh]$
Q_{Total}	$Total\ energy\ demand$ [kWh]
$RES_{Total,HP}$	$Renewable\ energy\ heat\ pump\ case$ [kWh]
$RES_{Total,Biomass}$	$Renewable\ energy\ biomass\ boiler\ case$ [kWh]
$C_{initial}$	$Initial\ investment\ cost\ [EUR]$
$C_{O,t}$	$Operational\ cost\ for\ the\ year\ t\ [EUR]$
$C_{M,t}$	$Maintenance\ cost\ for\ the\ year\ t\ [EUR]$
$C_{replacement,t}$	$Replacement\ cost\ for\ the\ year\ t\ [EUR]$
R_{end}	$Residual\ value\ an\ the\ end\ of\ the\ cycle\ [EUR]$
r	$Discount\ rate\ (reflecting\ the\ time\ value\ of\ money)$
n	$Total\ number\ of\ year\ in\ the\ life\ cycle$
PMV	$Predicted\ Mean\ Vote\ [-]$
PPD	$Predicted\ Percentage\ of\ Dissatisfied\ [-]$

References

1. Eurostat. Available online: https://ec.europa.eu/eurostat/web/interactive-publications/energy-2023 (accessed on 15 September 2024).
2. Papadopoulos, A.M. Fourty years of regulations on the thermal performance of the building envelope in Europe: Achievements, perspectives and challenges. *Energy Build.* **2016**, *127*, 942–952. [CrossRef]
3. Eurostat. Available online: https://ec.europa.eu/eurostat/ (accessed on 10 September 2024).
4. European Union. Directive (EU) 2023/2413 of the European Parliament and of the Council. *Official Journal of the European Union*, 18 October 2023.
5. Giama, E.; Kyriaki, E.; Fokaides, P.; Papadopoulos, A.M. Energy policy towards nZEB: The Hellenic and Cypriot case. *Energy Sources Part A Recovery Util. Environ. Eff.* **2021**, 1–14. [CrossRef]
6. European Union. Directive (EU) 2024/1275 of the European Parliament and of the Council on the energy performance of buildings (Recast). *Official Journal of the European Union*, 24 April 2024.
7. Giama, E.; Kyriaki, E.; Papaevaggelou, A.; Papadopoulos, A.M. Energy and Environmental Analysis of Renewable Energy Systems Focused on Biomass Technologies for Residential Applications: The Life Cycle Energy Analysis Approach. *Energies* **2023**, *16*, 4433. [CrossRef]
8. Lü, X.; Lu, T.; Karirinne, S.; Mäkiranta, A.; Clements-Croome, D. Renewable energy resources and multi-energy hybrid systems for urban buildings in Nordic climate. *Energy Build.* **2023**, *282*, 112789. [CrossRef]
9. Saffari, M.; Keogh, D.; De Rosa, M.; Finn, D.P. Technical and economic assessment of a hybrid heat pump system as an energy retrofit measure in a residential building. *Energy Build.* **2023**, *295*, 113256. [CrossRef]
10. Indepent Power Transmission System Operator (IPTO). Annual Press Release for 2023, Athens, 2024. (In Greek, Englisch Abstract). Available online: https://www.admie.gr/en/nea/deltia-typoy/2023-record-year-clean-energy-greece (accessed on 12 September 2024).

11. Jung, Y.G.; Lee, K.H.; Park, B.R.; Kim, T.W.; Moon, J.W. Development and performance evaluation of intelligent algorithm for optimal control of a hybrid heat pump system during the cooling season. *Energy Build.* **2024**, *306*, 113934. [CrossRef]
12. Chantzis, G.; Giama, E.; Nižetić, S.; Papadopoulos, A.M. The potential of demand response as a tool for decarbonization in the energy transition. *Energy Build.* **2023**, *296*, 113255. [CrossRef]
13. Daneshazarian, R.; Berardi, U. Nano-enhanced thermal energy storage coupled to a hybrid renewable system for a high-rise zero emission building. *Energy Convers. Manag.* **2023**, *291*, 117301. [CrossRef]
14. Wang, X.; Mi, Z.; Li, K.; Huang, X.; Bao, W.; Song, J.; Wang, C.; Chen, G.; Cao, P. Design and transient analysis of renewable energy-based residential net-zero energy buildings with energy storage. *Renew. Energy* **2024**, *220*, 119512. [CrossRef]
15. Cheraghi, R.; Jahangir, M.H. Multi-objective optimization of a hybrid renewable energy system supplying a residential building using NSGA-II and MOPSO algorithms. *Energy Convers. Manag.* **2023**, *294*, 117515. [CrossRef]
16. Jafarian, M.; Assareh, E.; Ershadi, A.; Wang, X. Optimal integration of efficient energy storage and renewable sources in hybrid energy systems: A novel optimization and dynamic evaluation strategy. *J. Energy Storage* **2024**, *101*, 113880. [CrossRef]
17. Skiadopoulos, A.; Kosmadakis, G.; van Heule, X.; Lecompte, S.; De Paepe, M.; Manolakos, D. Hybrid solar-biomass residential micro–Combined heat and power systems driven by the Partially Evaporating Organic Rankine Cycle—A case study in Southern Europe. *Therm. Sci. Eng. Prog.* **2024**, *55*, 102906. [CrossRef]
18. Official Journal of the European Uion. Available online: https://eur-lex.europa.eu (accessed on 10 September 2024).
19. Chatzikonstantinidis, K.; Giama, E.; Fokaides, P.A.; Papadopoulos, A.M. Smart Readiness Indicator (SRI) as a Decision-Making Tool for Low Carbon Buildings. *Energies* **2024**, *17*, 1406. [CrossRef]
20. Fokaides, P.; Papadopoulos, A.M. Cost-optimal insulation thickness in dry and mesothermal climates: Existing models and their improvement. *Energy Build.* **2014**, *68*, 203–212. [CrossRef]
21. *TOTEE 20701-3/2010*; Technical Instruction of the Technical Chamber of Greece. Ministry of Environment, Energy and Climate Change: Athens, Greece, July 2010. (In Greek)
22. Kaemmerlen, A.; Vo, C.; Asllanaj, F.; Jeandel, G.; Baillis, D. Radiative properties of extruded polystyrene foams: Predictive model and experimental results. *J. Quant. Spectrosc. Radiat. Transf.* **2010**, *111*, 865–877. [CrossRef]
23. *TOTEE 20701-1/2017*; Technical Instruction of the Technical Chamber of Greece. Ministry of Environment and Energy: Athens, Greece, September 2017. (In Greek)
24. Purdue University. Available online: https://engineering.purdue.edu (accessed on 25 August 2024).